

# Structural control of the São Francisco River Delta from the aeromagnetic data, Brazil.

---

## ABSTRACT

The São Francisco River delta is a Quaternary sandy plain built on a structural low of the Sergipe-Alagoas Basin, known as the São Francisco Low. The inner limit of the São Francisco River delta is defined by rectilinear cliffs between the delta plain and the Barreiras Formation, which coincide with important faults delimiting the São Francisco Low. Moreover, on the continental shelf, the deltaic clinoform developed over a topographic low limited by rectilinear scarps that present compatible orientation with the Sergipe-Alagoas structural framework. Thus, based on a theoretical background that indicates the existence of structural control over the formation of delta systems in general, and previous knowledge of this area, it is possible that the Sergipe-Alagoas Basin structure has influenced the delta. This relationship can be inferred using adequate methodology. Magnetometric data was integrated in the present study with the geological information on the area. The main objective was to evaluate the existing structural controls over the formation of the São Francisco delta and neighboring areas. The first stage of the present study consisted of a thorough bibliographic review and the search for pre-existing geophysical data in the region.

*Keywords: Delta; San Francisco; Aeromagnetic Data; Edge Detection.*

## 1. INTRODUCTION

Deltas are defined as a shoreline protuberance caused by the insertion of the fluvial system into a lower energy environment, in a context where the sedimentary supply is greater than the capacity of the basin to distribute ([2], [3]). Deltaic environments are of great importance since these areas offer various facilities for the populations that settle in them. As an example are the fertile land regions for agriculture, the proximity to river courses and the coastal zone [11].

Nowadays, many studies are carried out in deltas that target the oil and gas industry, but studies that are concerned with the environmental aspects of these regions have also been developed [11]. The significant increase in the environmental impacts caused by the increase of the population in these areas has generated an increasing concern with them, very susceptible to problems such as coastal erosion, subsidence, floods and salt intrusion [19].

There are several factors that are widely found in the literature, which are identified as those responsible for delta sedimentation: climate, river discharge, tidal amplitudes, wave energy, relative sea level variation, wind patterns ([4], [7], [8], [9]). Another important factor in the deltaic sedimentation is the tectonics of the area, which although little approached as one of the determining factors in this process presents evidences of its control in deltas around the world.

Some works present in the literature analyze the tectonics as the main controlling agent in the formation of the deltas. [Research by GOODBRED \*et al.\* \[12\]](#) on the Ganges-Brahmaputra delta, emphasized the influence of Himalayan tectonics on the sedimentation

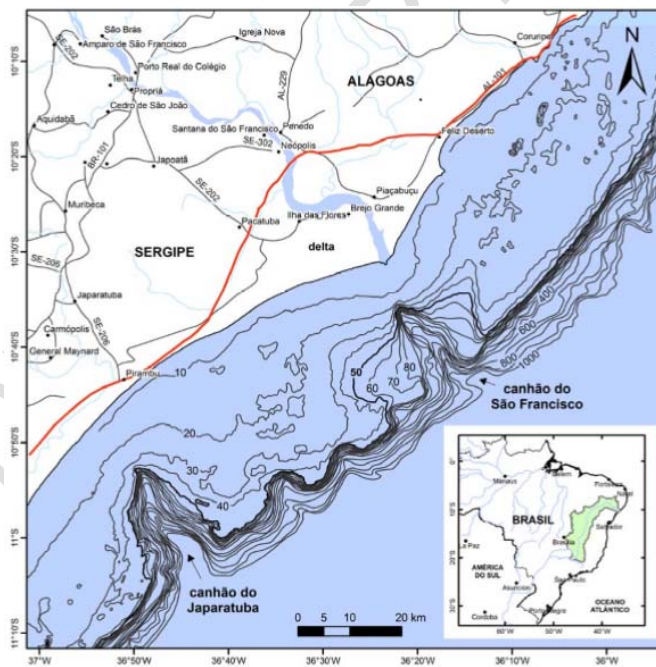
31 rates, magnitude and characteristics of the sedimentary deposits on the delta banks.  
32 **CARMINATI, MARTINELLI and SEVERI [5]** researched about the Pos Delta and the  
33 influence of glacial cycles and tectonic processes on the natural subsidence of this delta.

34 **ARMSTRONG et al. [1]** developed a study that shows the influence of the presence  
35 of reactivated growth faults in the Mississippi Delta, and **STANLEY [20]** developed a study  
36 that attempted to understand subsidence processes in the Nile Delta, where he concluded  
37 that subsidence rates were accelerated due to the neotectonic present in the region. Finally,  
38 **LIMA et al. [15]** researched the São Francisco Delta that focused on the study of the  
39 reactivation of faults in the Quaternary as the main controlling agent of sediment deposition  
40 and morphology of this delta.

41 The São Francisco River Delta (DSF) is a sandy, quaternary-level plain (Figure 1)  
42 built on a low basement of the Sergipe-Alagoas basin, known as Baixo do São Francisco  
43 [19]. Knowledge about DSF is basically restricted to its superficial outcrop portion.  
44 **GUIMARÃES [11]** was the first to provide subsurface information of the area, which allowed  
45 to advance in the knowledge of the depositional architecture of this system. A preliminary  
46 analysis of published works and existing data suggest some kind of tectonic control in the  
47 development of DSF.

48 The Sergipe-Alagoas Basin, located in the states of Sergipe and Alagoas, is  
49 distributed both on land and in the submerged region, extending towards the sea beyond the  
50 2,000 m isobath, in a total area of approximately 34,600 km<sup>2</sup>, being 12,000 km<sup>2</sup> in the  
51 emergent portion. This basin is limited by the parallels 9°S and 11°30'S and by the meridians  
52 34° 30'W and 37° 30'W.

53  
54



55

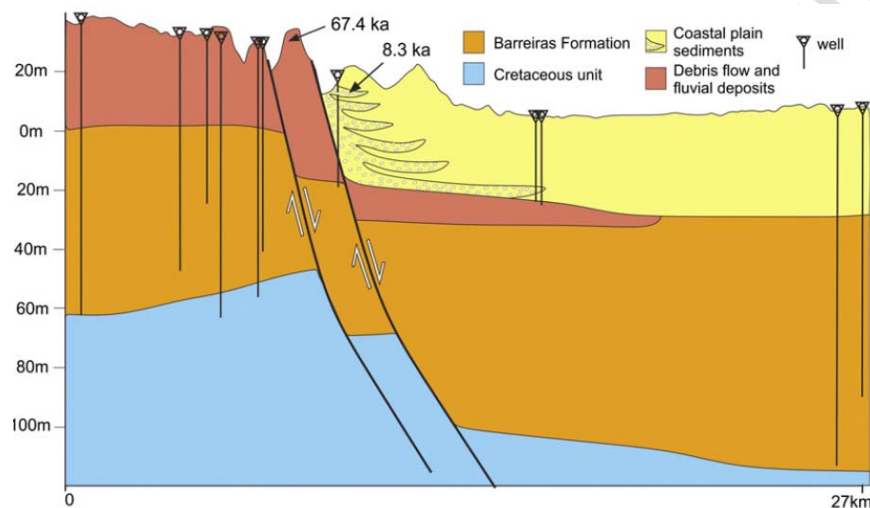
**Figure 1:** Location map of the study area. Source: [11].

56

57 In a more recent work, **LIMA et al. [15]** researched the DSF that had as main focus  
58 the process of reactivation of faults in the Quaternary, considered by the author as the main  
59 controlling agent of sediment deposition and delta morphology. This control would occur  
60 from the generation of new space for sediment accommodation, through the reactivation of  
61 faults. This work using well data, optical and radiocarbon dating and seismic data proposed

62 the existence. From three main stratigraphic units (Figure2): 1) Barreiras Formation deposits  
63 (fb) dated from the Miocene; 2) fluvial deposits and flow of debris (dff) dated to the Late  
64 Quaternary; 3) inter bedded braided stream (bsb) deposits also dated from the Late  
65 Quaternary. Data from pre-existing seismic surveys in the region show that the internal  
66 boundary of the DSF coincides with the N-S and NE-SW direction of Cretaceous faults.  
67 These faults form several cliffs and most of these are at the base of the uncontaminated  
68 sedimentary rocks of the fb and the dff unit.

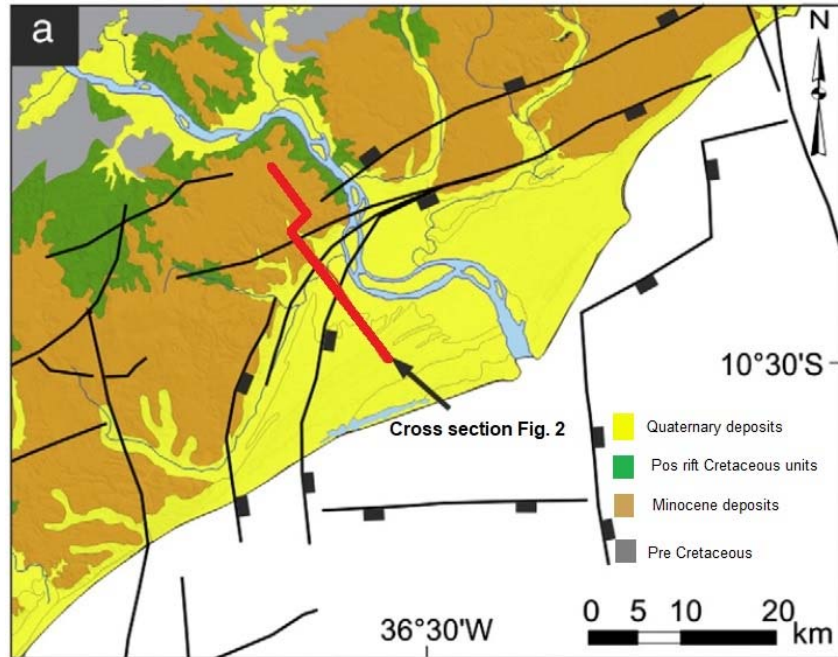
69  
70  
71  
72  
73  
74



75  
76  
77  
78  
79  
80  
81  
82  
83  
84  
85  
86  
87  
88  
89  
90  
91  
92  
93

**Figure 2:** Main stratigraphic units found in the area: 1) Barreiras Formation deposits (fb); 2) Fluid deposits and flow of debris (dff); 3) Braided stream (bsb) deposits according to LIMA et al. [15].

The author concludes that at least two major faults were reactivated during the Miocene. Figure 2 shows an increase in the thickness of the Barreiras Formation, crossing these faults, suggesting a sediment deposition contemporary to the failure processes, with reactivation of these faults during the Miocene. In Figure 3 it is possible to verify the Cretaceous faults with a parallel orientation to the internal boundary of the delta plain plunging toward the basin. LIMA et al. [15] also presented evidence of other reactivations during the Pleistocene-Holocene that affected or created additional accommodation space for the deposition of the other units. The Figure 3 shows the geological map evidencing the present failures in the region and the limits of the DSF.



94  
95  
96  
97

**Figure 3:** Simplified geological map evidencing the present failures in the region and the limits of the DSF. The cross section in red represents the section shown in Figure 2 (Source: [15]).

The present work consists in the use of the integrated magnetometry method to the geological data about the study area, having as main objective the evaluation of the structural controls in the formation and evolution of the DSF. While potential methods provide us with more general information on these controls, the seismic method is able to provide information in higher definition of subsurface geological features.

It consists of the interpretation of maps generated from the aeromagnetic data, such as the Map of the Tilt Angle of the Horizontal Total Gradient (TAHG) that allows us to visualize in subsurface the presence of magnetic bodies and their contacts, besides the generation of a quantitative solution in depth. Magnetic maps are frequently used to delineate geologic contacts and border of geological formation. These maps have signals with various amplitudes that originate from different geometric sources, situated at different depths and with different magnetic properties.

98  
99

## 2. MAGNETOMETRIC METHOD

100 The development of the databases involved merging numerous surveys with  
101 aeromagnetic data with highly variable specifications and quality [6]. The integrated and  
102 corrected anomaly maps were processed and interpreted. Knowing the magnetic anomaly it  
103 was possible to estimate the depth top and bottom, magnetic lineaments, faults, blocks, the  
104 lateral extension, the width of the sources. From these results, we can produce a geological  
105 interpreting and understanding the tectonic environment. For regional exploration, magnetic  
106 measurements were important for example, continental boundaries of terrain were  
107 commonly recognized by magnetic contrast in all contact. Such regional interpretations  
108 required continental scale for magnetic databases.

109 The magnetometry data used in this work belong to the database of CPRM (Mineral  
110 Resources Research Company) and was assigned to this study by the Laboratory of Nuclear

111 Physics and Environment of the Federal University of Bahia. The data includes two  
112 aeromagnetic surveys carried out in the region encompassing the Deltaic Plain of the São  
113 Francisco River belonging to the projects 1102\_ESTADO\_DE\_SERGIPE and  
114 11\_04\_PAULO\_AFONSO\_TEOTÔNIO\_VILELA (Figure 4).

115

116 The aeromagnetic projects have a spacing of flight lines of 500 m oriented in the N-  
117 S direction, with flight height of 100 m, the interval between measurements of the  
118 magnetometer of 0.1 s and the spectrometer 1.0 s. The survey was carried out in two  
119 different blocks with different flight and tie-line directions, and data acquisition was  
120 performed perpendicular to the main structures of the surveyed area [6]. The magnetic data  
121 of the study area generated from the pre-processed data, using different combinations of  
122 parameters, the cell size of 1/4 of the flight line. Grids of the magnetic anomaly were  
123 generated and then a database of each grid generated around the Sergipe-Alagoas Basin  
124 defining the study area. The magnetic system used was an optically pumped (cesium vapor)  
125 magnetometer that was installed in a stinger extension behind the tail of the aircraft. The  
126 output from the magnetometer was sampled at 0.1 s to a resolution of 0.001 nT with a noise  
127 envelope less than 0.01 nT.

128

129 In the next processing step, the data were interpolated to a regular grid, using  
130 algorithms that maintain data fidelity at the original measurement locations. This step was  
131 followed by correction of spurious effects caused by the leveling of the original grids. The  
132 fourth-order difference technique was used to track anomalous spikes in the magnetic data  
133 and to condition sampling along the flight lines based on the spatial Nyquist frequency. This  
134 was performed on the selected interpolated grid, which contained square cells 125 x 125 m.  
135 The algorithm was based on linear interpolation along the direction of the flight lines, and on  
136 the Akima spline perpendicular to the flight lines. Microleveling and decorrugation techniques  
137 were applied to the data. This procedure resulted in several geophysical data products,  
138 including thematic maps of both individual variables and composite variables, for use in  
139 geologic analysis and interpretation.

140

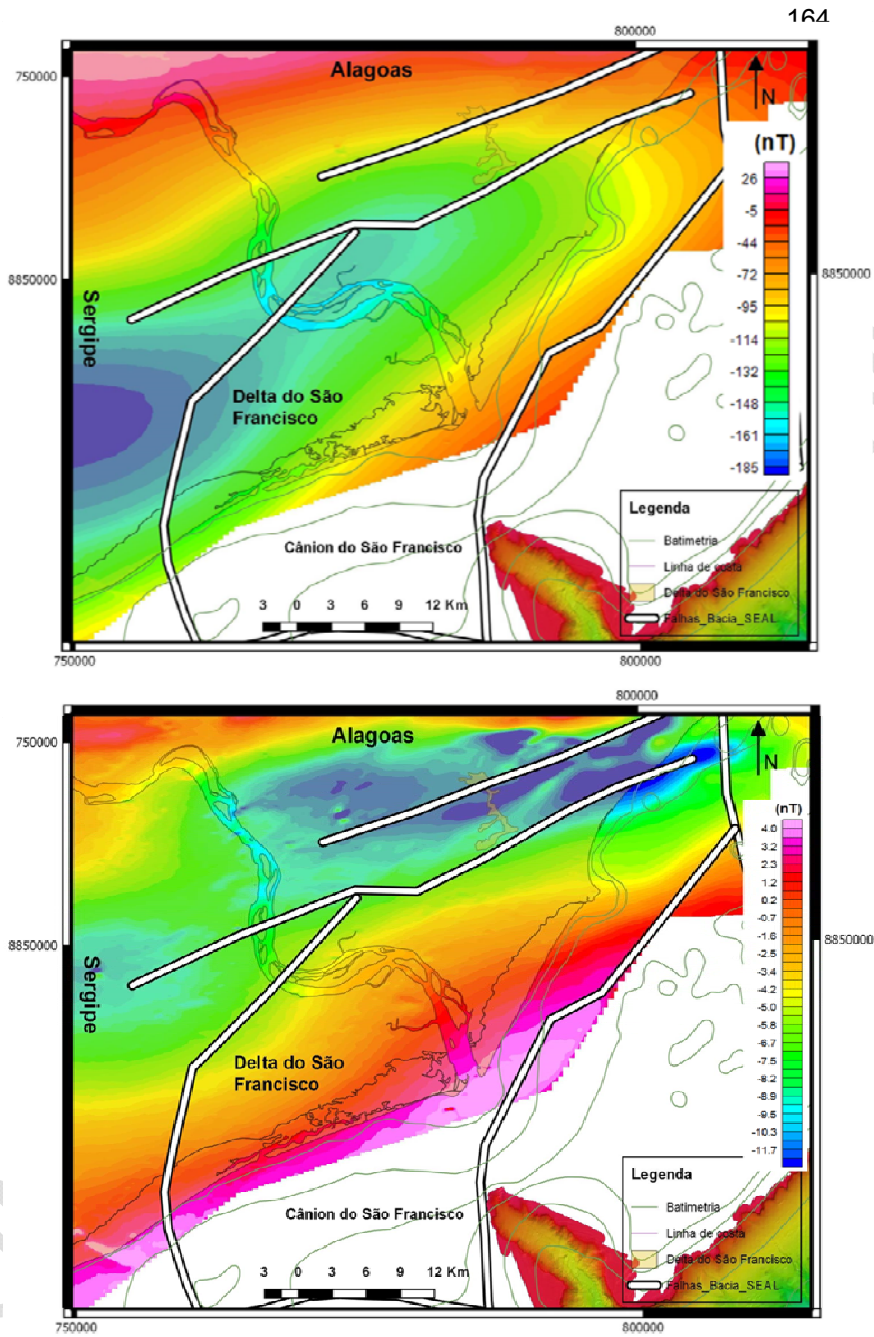
141 Usual linear transformations were applied to the magnetic data to process changes  
142 in the amplitude and/or phase related to the set of the data [14]. These transformations are  
143 carried out by multiplying the Fourier transform in the data set in the frequency domain. The  
144 inverse Fourier transform returns to the space domain and gives the current field to the  
145 upper level. This is equivalent to convolving the field in the space domain by an operator (or  
146 filter). All transformations of the magnetic field work on this path. For the magnetic data  
147 processing, a regional-residual separation process was required to obtain the subject of  
148 interest of this study. To do so, an upward continuation was performed, where the estimated  
149 depth value used in this process was obtained through radially average power spectrum  
150 analysis of the magnetic data.

150

151 The aeromagnetic data assigned to this work was in its raw state and its treatment  
152 followed a characteristic route: application of the equation reduction filter of the anomalous  
153 magnetic field data, power spectrum analysis and regional-residual separation from  
154 upwards. The calculation of the field at higher levels is called continuation upwards and  
155 proposes the removal of high frequency anomalies relative to low frequency anomalies.

155

156 After the Total Magnetic Field (TMF) data was reduced to the Equator, two  
157 ascending continuations were applied, one for 100 m and the other for 1000 m, which were  
158 defined from the power spectral study of the magnetic signal. The first allowed the removal  
159 of low frequencies that are characterized by superficial noises and the second allowed the  
160 elimination of deeper frequencies. The grids generated in both processes were subtracted  
161 (regional / residual separation) so that the resulting magnetic information is related only to  
162 geological features that extend up to approximately 1000 m depth. The gross TMF and TMF  
maps after the RE and CA steps are shown in Figures 4a and 4b.



208  
209  
210

**Figure 4:** A) TMF map; B) and TMF map reduced to the equator and continued upward with regional / residual subtraction.

211 FERREIRA *et al.* [10] presented an edge detection method that is based on the  
212 enhancement of the THG of magnetic anomalies using the Tilt Angle. It is referred to as the  
213 tilt angle of the horizontal gradient (TAHG). In this study, efficiency of the TAHG is  
214 considered for magnetic data set. The TAHG transform range is from  $-\pi/2$  to  $+\pi/2$  (Figure 5).

215 From this, some enhancement methods were used that gave rise to the Analytical  
216 Signal Anomaly (ASA), Total Horizontal Gradient (THG), and Total Horizontal Gradient  
217 Analytical Signal Slope (TAHG) maps. Both enhancements are best described below.

218  
219 1) Amplitude of the Signal Analytic (ASA): Asymmetric function in bell format that  
220 aims to delimit magnetic bodies and to centralize them above their sources [13]. The ASA  
221 map represents magnetic anomalies free of noise and the influence of deep sources.

222 2) Total Horizontal Gradient (THG): A highlight technique that allows  
223 distinguishing the lateral boundaries of anomalous sources through abrupt changes in the  
224 physical properties of lithology. In the THG map the maximum values of the anomalies are  
225 located on the edge of the anomalous source.

226 3) Total Total Horizontal Gradient Analytical Signal Slope (TAHG): TAHG  
227 enhances GHT through subsequent application of analytic signal slope [10]. The method  
228 centralizes the maximum amplitude at the edges of the magnetic sources and different from  
229 the GHT is not related to the depth of the same.

230 In addition to the corrections and the generation of the enhancement maps that  
231 characterize a qualitative data analysis, quantitative solutions were also generated from the  
232 SPI method. The SPI method calculates three attributes of the Complex Analytical Signal,  
233 amplitude, phase and local frequencies, which allow us to calculate the Local Probability  
234 Depth, Diving and Contrast parameters of the magnetic sources ([16], [21]).

235

236

### 237 3. RESULTS AND DISCUSSION

238

239 The methods were used that gave rise to the Analytical Signal Anomaly (ASA), Total  
240 Horizontal Gradient (THG), and Total Horizontal Gradient Analytical Signal Slope (TAHG)  
241 maps. The Figure 5 shows respectively the ASA, THG, TAHG and SPI solution maps.

242

243 Then analysis of all products generated with the magnetic data was performed and  
244 the maps chosen for joint interpretation were: TMF reduced to the equator and continued  
245 upwards, TAHG and map with SPI in-depth solution. In the TMF map (Figure 6) it was  
246 possible to individualize the main magnetic regions of the study area:

247

- 248 1) Region of very low magnetic amplitudes; F.
- 249 2) Region of low magnetic amplitudes;
- 250 3) Region of intermediate magnetic amplitudes; D.
- 251 4) Region of high magnetic amplitudes: C.
- 252 5) Regions of very high magnetic amplitudes: A, B.

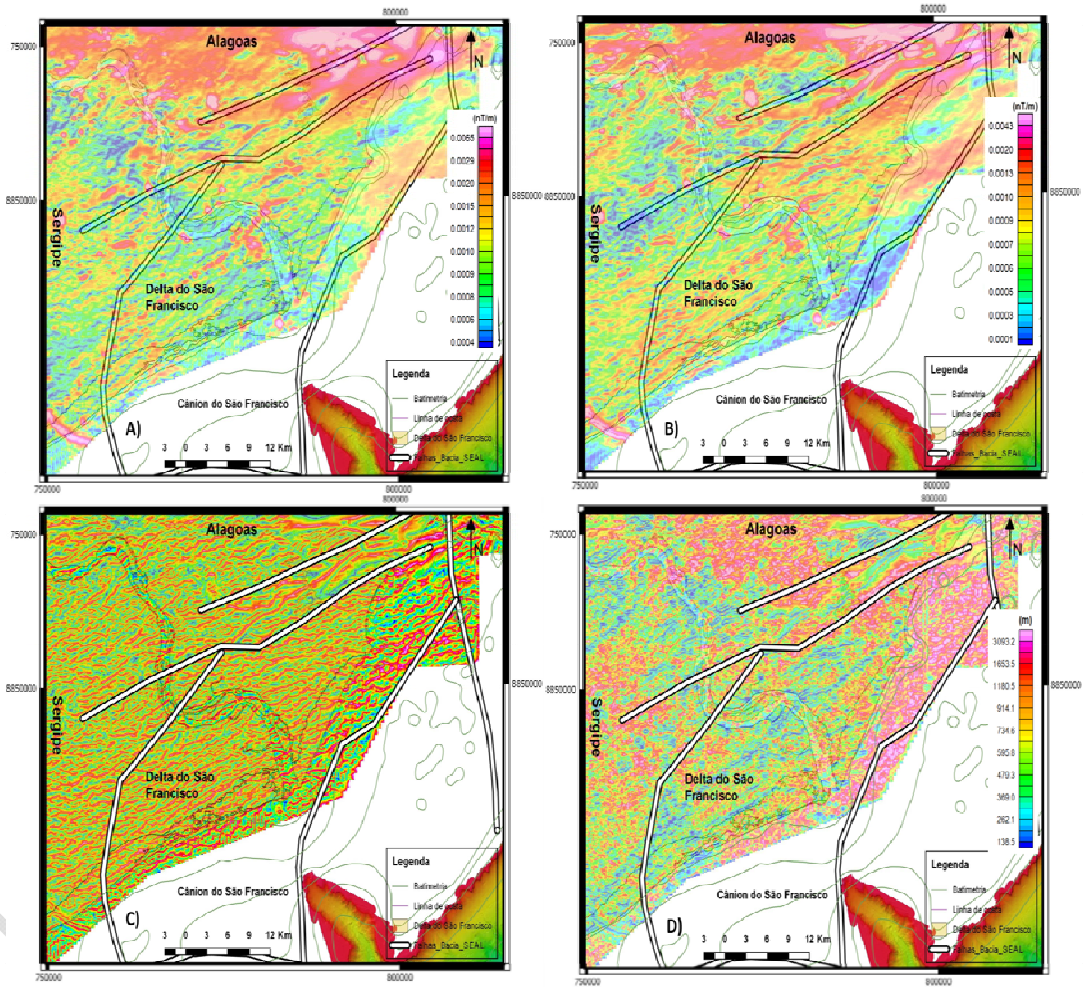
253

254 With respect to the TMF map and its magnetic regions, it is possible to observe that  
255 there is a tendency in the increase of the magnetic field when approaching the coastline,  
256 expected factor since the sea behaves like a great conductor and influences positively in the  
257 values from Camp. The regions E and F characterized as zones of low and very low  
258 magnetic field, respectively, may be associated to existing depocenters within the Sergipe-  
259 Alagoas basin, since a large column of sedimentary material would increase the distance to  
260 the basement of the basin and present smaller values of magnetic field.

261 The TAHG map (Figure 7) was interpreted and the main magnetic lineaments of the  
262 study area were duly marked. The joint analysis of this interpretation with the map of the SPI  
263 solution (Figure 8) allowed us to individualize the bodies and their respective depths.

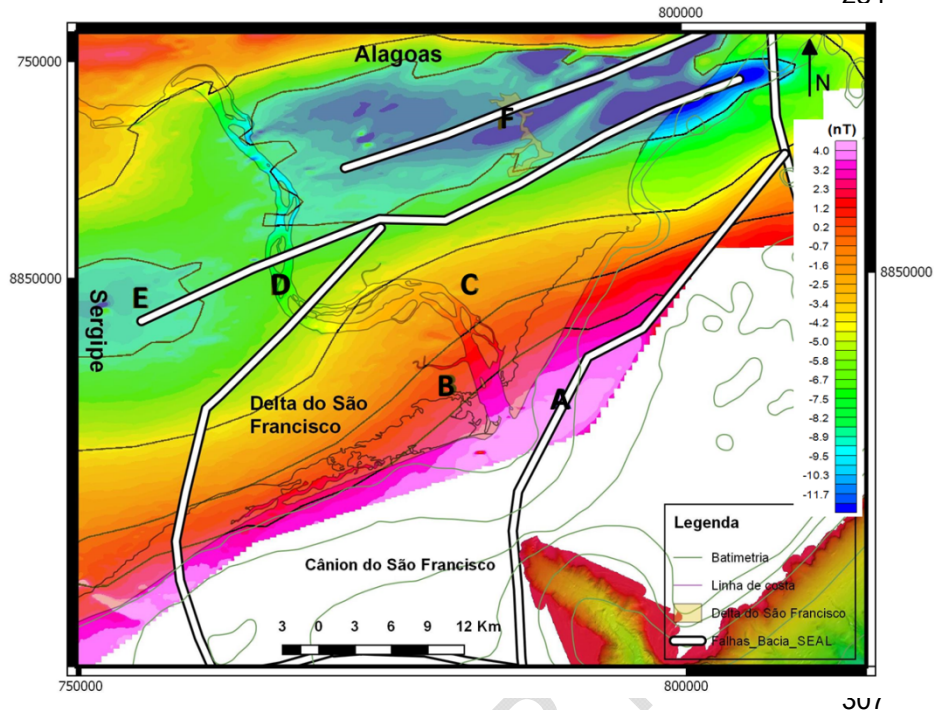
264 Another important feature observed in the map interpreted TAHG is the preferred direction of  
265 the magnetic lineaments. These, in turn, have preferential directions NE-SW and E-W, in  
266 addition to some NW-SE perpendicular structures. These directions coincide with the tracing  
267 of the main flaws that constitute the structural framework of the Sergipe-Alagoas basin.

268 Based on depth information obtained in the SPI solution map, it is possible to verify  
269 that the interpreted magnetic lineaments, which in turn may correspond to contact regions or  
270 faults, on the TAHG map are at a maximum depth of about 1200 m, which leads us to  
271 suggest that the faults in the structural framework of the SE-AL basin, which are deeper,  
272 have an extension to shallower regions.  
273  
274



275  
276  
277 **Figure 5:** A) ASA map; B) Map of THG; C) TAHG Map; D) Map of SPI.  
278  
279  
280  
281  
282  
283





308 **Figure 6:** Map of TMF reduced to the equator and continued upward with its main  
 309 individualized magnetic regions.

310 On the magnetic information obtained in this work, we have the maps of TAHG  
 311 (Figure 7) and the SPI depth solution (Figure 8) superimposed on the study area. It was  
 312 previously highlighted the existence of a preferential direction of the magnetic lineaments  
 313 found in the region, they are parallel or subparallel to important flaws that delimit the  
 314 structural framework of the SE-AL basin. Note that the magnetic lineages on the DSF are  
 315 very shallow when observing the depth values of the region on the SPI map, which  
 316 suggests that they may be the expression of coastal strands in the delta plain.

317 Another important point to note is the marking of the magnetic lines that delimit the San  
 318 Francisco low on the TAHG map (area 1 and 2 on the map). The blue lineages on the map  
 319 (Figures 7 and 8) were interpreted as the region of rectilinear cliffs belonging to the  
 320 Barreiras Formation and are the internal boundaries of the deltaic plain with formation. Note  
 321 that these cliffs accompany the tracing of lineages belonging to the SE-AL basin, which,  
 322 according to Ponte [17], shows a direct influence of the basin structuring on the formation of  
 323 the DSF. Another important aspect to be noticed is the regions A and B, of the SPI solution  
 324 map, which present higher values of depth and continue to reinforce the idea of the  
 325 presence of depocenters of the basin.

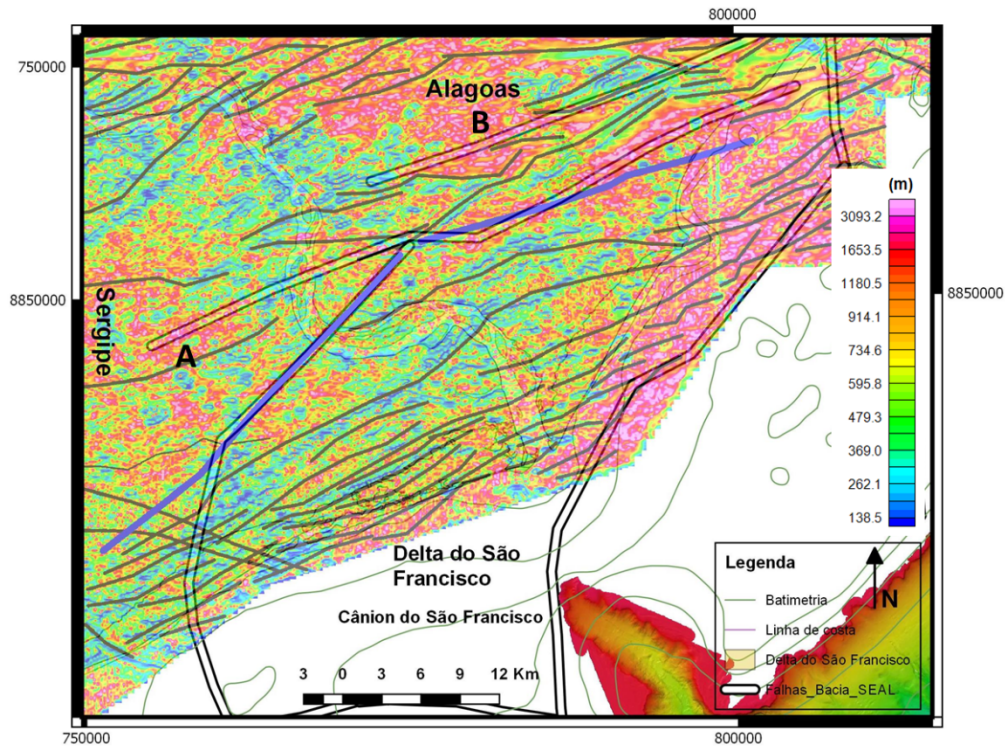
326

327 It was possible to identify, from the joint analysis of all the information generated  
 328 and pre-existing, the presence of a set of faults that directly affect the sedimentation in the  
 329 region. However, previous knowledge of the geology of the area leads us to believe that the  
 330 observed faults would not be related to a possible reactivation of tectonic character, but to  
 331 processes that involve material overload and consequent gravitational collapse of the region  
 332 being studied.

333

334

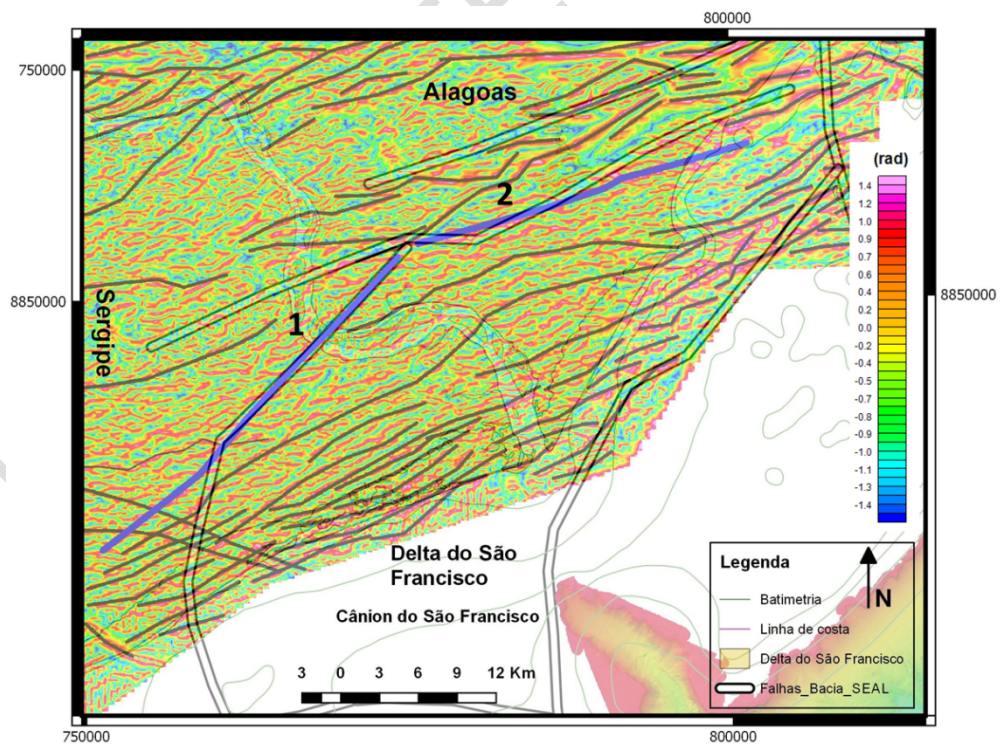
335



**Figura**

360 **re 7:** Interpreted TAHG map. The lines marked in black represent the marked magnetic  
 361 lineaments and the blue lines the deltaic plain with the Barreiras Formation.  
 362  
 363

364  
 365  
 366  
 367  
 368  
 369  
 370  
 371  
 372  
 373  
 374  
 375  
 376  
 377  
 378  
 379  
 380  
 381  
 382  
 383  
 384  
 385  
 386  
 387



388 **Figure 8:** SPI solution map. The lines marked in black represent the marked magnetic  
389 lineaments and the blue lines the deltaic plain with the Barreiras Formation.  
390

#### 391 **4. CONCLUSION**

392 The present work presents the results of a joint analysis of magnetic data and previous  
393 geological and geophysical information of the area comprising the DSF and its environment.  
394 There has been an attempt to understand the structural controls that affect the origin and  
395 evolution of the delta, whether these controls are associated with a new tectonic present in  
396 the region and whether the structuring of the SE-AL basin also exerts some influence. The  
397 treatment and interpretation of the aeromagnetic data provided us with a design of the  
398 magnetic framework of the region, where it was possible to show the main lineaments in the  
399 area. It was also possible through the magnetic die to mark the inner boundary of the delta  
400 plain. Thus, the greatest contribution of this method was to the information on the geological  
401 aspect of the area, which together with the Bouguer anomaly map of the region provided us  
402 with more precision, the expression of coastal strands presents in the delta sedimentation,  
403 the marking of possible depocenters of the basin and the limits of the delta. It was not  
404 possible to identify in this work the presence of a more recent and active tectonic in the  
405 region, so the origin of the failures that exert a structural control in the area can be  
406 associated with mass gravitational collapses driven by the overload of material deposited in  
407 the region.

408

409

#### 410 **ACKNOWLEDGEMENTS**

411

412 We are grateful to the CPRM (Brazilian Geology Program) for the Aerogeophysical  
413 Projects for granting the data used in this work.

414

415

416

#### 417 **REFERENCES**

418

419 1. ARMSTRONG C., MOHRIG D., HESS T., GEORGE T., STRAUB K. M., 2014. Influence  
420 of growth faults on coastal fluvial systems: Examples from the late Miocene to Recent  
421 Mississippi River Delta, *Sedimentary Geology* 301, 120–132.

422

423 2. BITTENCOURT, A.C.S.P.; DOMINGUEZ, J.M.L.; FONTES, L.C.S.; SOUSA, D.L.; SILVA,  
424 I.R.; SILVA, F.R., 2007. Wave refraction, river damming, and episodes of severe shoreline  
425 erosion: the São Francisco river mouth, northeastern Brazil. *Journal of Coastal Research*. 23  
426 (4), p. 930-938.

427

428 3. BHATTACHARYA, J.P.; GIOSAN, L., 2003. Wave-influenced deltas: geomorphological  
429 implications for facies reconstruction. *Sedimentology*. 50, p.187-210.

430

431 4. BHATTACHARYA, J. P.; WALKER, R. G., 1992. Deltas. In: WALKER, R. G.; JAMES, N.  
432 P. (eds.): *Facies Models - Response to sea level change*. Toronto. Geological Association of  
433 Canada, p. 157-178.

434

435 5. CARMINATI, E., MARTINELLI, G., and SEVERI, P., 2003, Influence of glacial cycles and  
436 tectonics on natural subsidence in the Po Plain (Northern Italy): Insights from 14C ages:  
437 *Geochemistry, Geophysics, Geosystems*, v. 4, p. 1082.

438

- 439 6. CPRM, 2008. Projeto Aerogeofísico Borda Leste do Planalto da Borborema, CPRM  
440 (Programa Geologia do Brasil).  
441
- 442 7. DOMINGUEZ, J.M.L., 1990. Delta dominados por ondas: críticas às idéias atuais com  
443 referência particular ao modelo de Coleman & Wright. *Revista Brasileira de Geociências*, 20  
444 (1-4), p. 352-361.  
445
- 446 8. DOMINGUEZ, J.M.L., 1996. The São Francisco strand plain: a paradigm for wave-  
447 dominated deltas. *Geological Society Special Publication* 117: 217-231.  
448
- 449 9. DOMINGUEZ, J.M.L.; BITTENCOURT, A.C.S.P; MARTIN, L., 1981. O papel da deriva  
450 litorânea de sedimentos arenosos na construção das planícies costeiras associadas às  
451 desembocaduras dos rios São Francisco (SE-AL), Jequitinhonha (BA), Doce (ES) e Paraíba  
452 do Sul (RJ). *Revista Brasileira de Geociências*. 13(2). 1983. p. 98-105.  
453
- 454 10. FERREIRA, F. J. F.; de SOUZA, J.; de BARROS, A.; BONGIOLO, S.; de CASTRO, L. G.  
455 e ROMEIRO, M. A. T., 2010. Realce do gradiente horizontal total de anomalias magnéticas  
456 usando a inclinação do sinal analítico. parte I-aplicação a dados sintéticos, In:IV Simpósio  
457 Brasileiro de Geofísica.  
458
- 459 11. GUIMARÃES, J.K., 2010. Evolução do delta do rio São Francisco – estratigrafia do  
460 Quaternário e relações morfodinâmicas. Tese (Doutorado em Geologia) - Universidade  
461 Federal da Bahia. Instituto de Geociências. Orientador: José Maria Landim Dominguez.  
462 2010. 127 p.  
463
- 464 12. GOODBRED, S.L., Jr., KUEHL, S.A., STECKLER, M.S., and SARKER, M.H., 2003.  
465 Controls on facies distribution and stratigraphic preservation in the Ganges-Brahmaputra  
466 delta sequence: *Sedimentary Geology*, v. 155, p. 301–316.  
467
- 468 13. GUNN, P.J., 1997. Quantitative methods for interpreting aeromagnetic data: a subjective  
469 review. *Journal of Australian Geology & Geophysics*, v.17, n.2, p. 105-113.  
470
- 471 14. Hood, P.J. and Teskey, D.J., 1989. Aeromagnetic gradiometer program of the Geological  
472 Survey of Canada. *Geophysics*, 54 (8), 1012–1022.  
473
- 474 15. LIMA, C.U., BEZERRA, H.R., NOGUEIRA, C. C., RUBSON, P., SOUZA, O.L., 2014,  
475 Quaternary fault control on the coastal sedimentation and morphology of the São Francisco  
476 coastal plain, Brazil. *Tectonophysics*, 633, 98-114.  
477
- 478 16. NABIGHIAN, M. N., 1972. The analytic signal of two-dimensional magnetic bodies with  
479 polygonal cross-section: Its properties and use for automated anomaly interpretation,  
480 *Geophysics*, 37(1):507-517.  
481
- 482 17. PONTE, F.C. (1969), **Estudo Morfo-Estrutural da Bacia Alagoas-Sergipe – Bol. Tec.**  
483 **Petrobras 12 (4): 439, 474.**
- 484
- 485 18. SÁNCHEZ-ARCILLA, A.; JIMENÉZ, J.A.; VALDEMORO, H.I., 1998. The Ebro delta:  
486 morphodynamics and vulnerability. *Journal of Coastal Research* 14 (3): 754–772.  
487
- 488 19. SOUZA-LIMA, W. Litoestratigrafia e evolução tectono-sedimentar da bacia de Sergipe-  
489 Alagoas, introdução. *Fundação Paleontológica Phoenix*. Aracaju. Ano 8. n. 89. 2006.  
490

- 491 20. STANLEY D.J., 1988, Subsidence in the northeastern Nile delta: Rapid rates, possible  
492 causes, and consequences: Science, v. 240, p. 497–500.  
493
- 494 21. THURSTON, J. B. e Smith, R. S., 1997. Automatic conversion of magnetic data to  
495 depth, dip, and susceptibility contrast using the SPI (tm) method, Geophysics, 62(3):807.

UNDER PEER REVIEW